

*Supporting Information for*

**Rational Design of Porous Sn Nanospheres/N-Doped Carbon Nanofibers as An**

**Ultra-Stable Potassium-Ion Battery Anode Material**

Chao Li, An Tong Bi, Hong Li Chen, Ya Ru Pei, Ming Zhao, Chun Cheng Yang,\* Qing Jiang\*

---

*Key Laboratory of Automobile Materials (Jilin University), Ministry of Education, and School of Materials Science and Engineering, Jilin University, Changchun 130022, China*

*\* Corresponding authors. Tel.: +86-431-85095371; Fax: +86-431-85095876; E-mails: ccyang@jlu.edu.cn (C. C. Yang); jiangq@jlu.edu.cn (Q. Jiang).*

*† Electronic Supplementary Information (ESI) available. See DOI: 10.1039/x0xx00000x*

## Materials and methods

*Chemicals:* Tin (IV) chloride pentahydrate ( $\text{SnCl}_4 \cdot 5\text{H}_2\text{O}$ , 99.995%, Shanghai Macklin Biochemical Co., Ltd), cobalt (II) chloride hexahydrate ( $\text{CoCl}_2 \cdot 6\text{H}_2\text{O}$ ,  $\geq 99.0\%$ , Sinopharm Chemical Reagent Co., Ltd), sodium citrate anhydrous ( $\text{C}_6\text{H}_5\text{Na}_3\text{O}_7$ , 98%, Ourchem), sodium hydroxide ( $\text{NaOH}$ ,  $\geq 96.0\%$ , Sinopharm Chemical Reagent Co., Ltd), ethanol ( $\text{C}_2\text{H}_5\text{OH}$ , 99.7%, Beijing Chemical Works), nitric acid ( $\text{HNO}_3$ , 65~68%, Aladdin Reagent Co., Ltd), N, N-dimethylformamide ( $\text{C}_3\text{H}_7\text{NO}$ ,  $> 99.9\%$ , Aladdin Reagent Co., Ltd), polyacrylonitrile [ $(\text{C}_3\text{H}_3\text{N})_n$ , average molecular weight 150,000, Shanghai Macklin Biochemical Co., Ltd], iron (III) chloride hexahydrate ( $\text{FeCl}_3 \cdot 6\text{H}_2\text{O}$ ,  $\geq 99.0\%$ , Sinopharm Chemical Reagent Co., Ltd), potassium ferricyanide [ $\text{K}_3\text{Fe}(\text{CN})_6$ , 99.95%, Aladdin Reagent Co., Ltd], Ar/ $\text{H}_2$  gas mixture (90 vol.% Ar and 10 vol.%  $\text{H}_2$ ). All the chemicals were used without further purification. The deionized water used in all experiments was with a specific resistance of 18.2  $\text{M}\Omega \cdot \text{cm}$ .

*Preparation of porous  $\text{SnO}_2$ :*  $\text{CoSn}(\text{OH})_6$  nanocrystals were prepared by using a method reported in the literature.<sup>1</sup> For preparing porous  $\text{SnO}_2$ , the as-prepared cubic  $\text{CoSn}(\text{OH})_6$  was annealed at 700 °C in air for 3 h, followed by  $\text{HNO}_3$  etching (30 mL, 3 M).<sup>2</sup> The etching process was carried out in a Teflon-lined autoclave at 140 °C for 5 h. Finally, the porous  $\text{SnO}_2$  powder was obtained after washing, centrifuging and drying.

*Preparation of Sn/N-CNFs:* First, porous SnO<sub>2</sub> and PAN were mixed together with a weight ratio of 5:6 in DMF solution, and stirred at 60 °C for 12 h. Then, the SnO<sub>2</sub>/PAN nanofibers were prepared by electrospinning the precursor solution under a voltage of 18 kV with a feeding rate of 1 mL h<sup>-1</sup>. The distance between the collector and the stainless steel needle was fixed at 18 cm. After that, SnO<sub>2</sub>/PAN nanofibers were stabilized at 250 °C for 3 h in air, and then annealed at 500 °C for 1, 5, 20 and 120 min, respectively, with a heating rate of 1 °C min<sup>-1</sup> in Ar/H<sub>2</sub> to obtain the samples of Sn/N-CNFs-1, Sn/N-CNFs-5, Sn/N-CNFs-20 and Sn/N-CNFs-120. 60%-Sn/N-CNFs-5 was obtained by increasing the weight ratio of the precursors of porous SnO<sub>2</sub> to polyacrylonitrile (PAN) (3:2) with a similar procedure as fabricating Sn/N-CNFs-5. Moreover, N-CNFs-1, N-CNFs-5, N-CNFs-20 and N-CNFs-120 were prepared by regulating the calcination time (1, 5, 20 and 120 min, respectively) of the precursors of PAN with a similar procedure as fabricating Sn/N-CNFs-5 without adding porous SnO<sub>2</sub>.

*Preparation of KPBNPs:* KPBNPs were synthesized by using a reported method in the open literature.<sup>3</sup> In a typical preparation, 1 mmol K<sub>4</sub>Fe(CN)<sub>6</sub> was dissolved in 160 mL deionized water to form a homogeneous solution (noted as A solution). 2 mmol FeCl<sub>3</sub>·6H<sub>2</sub>O was added in 40 mL deionized water to form a uniform solution (noted as B solution). B solution was added into A solution drop by drop under stirring and the

precipitation occurred immediately. The mixture was agitated for 2 h and allowed to stand for another 24 h. KPBNPs were collected by centrifugation, washed by water and ethanol, and dried at 80 °C in a vacuum oven for 24 h.

*Materials Characterization:* The morphology and microstructure of the samples were acquired by FESEM (JSM-6700F, JEOL, 15 kV) and TEM (JEM-2100F, JEOL, 200 kV). XRD measurements were carried on a D/max2500pc diffractometer using Cu-K $\alpha$  radiation ( $\lambda = 0.15406$  nm). XPS spectra were collected on an ESCALAB 250 spectrometer (Thermo Fisher Scientific, UK) by using a monochromatic Al-K $\alpha$  (1486.6 eV) source. Raman spectra were obtained using a micro-Raman spectrometer (Renishaw) with a 532 nm laser. TGA was conducted in air using an SDT Q600 instrument with a heating rate of 5 °C min<sup>-1</sup> over 50-800 °C. The specific area and pore size distribution were determined by nitrogen adsorption and desorption using a Micromeritics ASAP 2020 analyzer.

*Electrochemical Measurements:* The working electrodes were made by mixing 70% active materials, 15% Super P and 15% sodium carboxymethyl cellulose (Na-CMC) in deionized water. The obtained slurry was pasted on a Cu foil and dried at 60 °C for 12 h in vacuum. Then the working electrodes were punched out with a diameter of 12 mm with the mass loading of 0.5-1 mg for active materials. The K-ion half cells (CR2025) were assembled in an Ar-filled glove box ([O<sub>2</sub>] < 1 ppm, [H<sub>2</sub>O] < 1 ppm)

using as-synthesized materials as the working electrode, potassium foil as a counter/conference electrode and glass fiber (GF/D) as the separator. The electrolyte was composed of 0.8 M KPF<sub>6</sub> dissolved in a mixture of ethylene carbonate and diethyl carbonate with a volume ratio of 1:1. The galvanostatic discharge/charge cycling tests were performed using a LAND CT2001A battery testing system in the voltage range between 0.01 and 3.0 V. CV measurements were recorded on an Ivium-n-Stat electrochemical workstation (Ivium Technologies) with a potential scan rate of 0.1 mV s<sup>-1</sup> between 0.01 and 3.0 V. EIS measurements were conducted by applying an amplitude of 10 mV over the frequency range from 100 kHz to 10 mHz. To test the cycled electrodes, the electrodes were disassembled from the cells in an argon-filled glove box ([O<sub>2</sub>] < 1 ppm and [H<sub>2</sub>O] < 1 ppm) followed by washing the electrodes with dimethyl carbonate to remove the potassium salt before *ex-situ* characterization. For the full cells, the cathode electrodes were prepared by mixing 70% KPBNPs, 20% Super P and 10% binder (PVDF) with N-methyl-2-pyrrolidone (NMP) as the solvent, which were pasted on Al foil and dried in vacuum at 110 °C for 12 h. The full cells were constructed by using KPBNPs as the cathode and Sn/N-CNFs as the anode. The mass ratio between cathode and anode is controlled to be 2:1. Meanwhile, the Sn/N-CNFs electrode was pre-activated for three cycles at a current density of 0.1 A g<sup>-1</sup> in the half cells before the assembly of potassium-ion full cells. As an example, the discharge and

charge measurements of full cell were tested on the LAND CT2001A battery testing system in the voltage range of 1-3.8 V (based on the active material mass of the anode).

Supplementary Figures

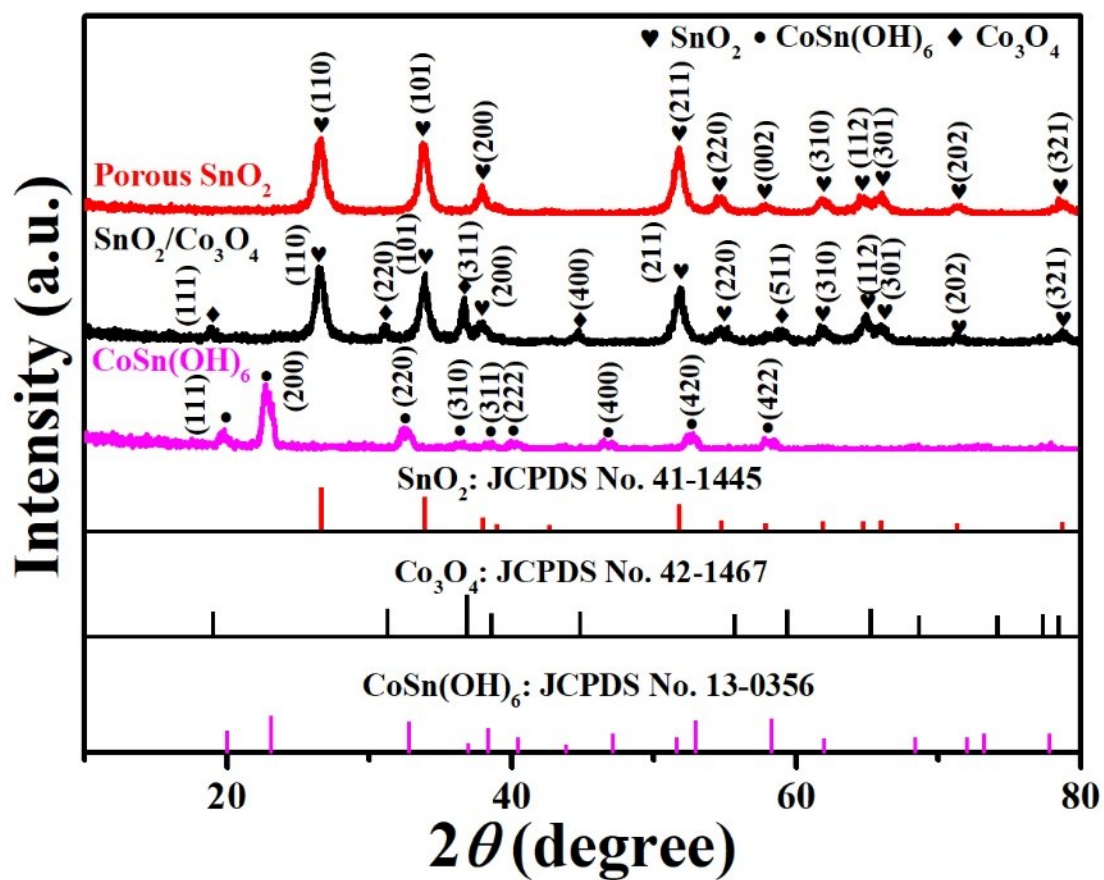


Fig. S1. XRD patterns of intermediate products of CoSn(OH)<sub>6</sub>, SnO<sub>2</sub>/Co<sub>3</sub>O<sub>4</sub> and porous SnO<sub>2</sub>.

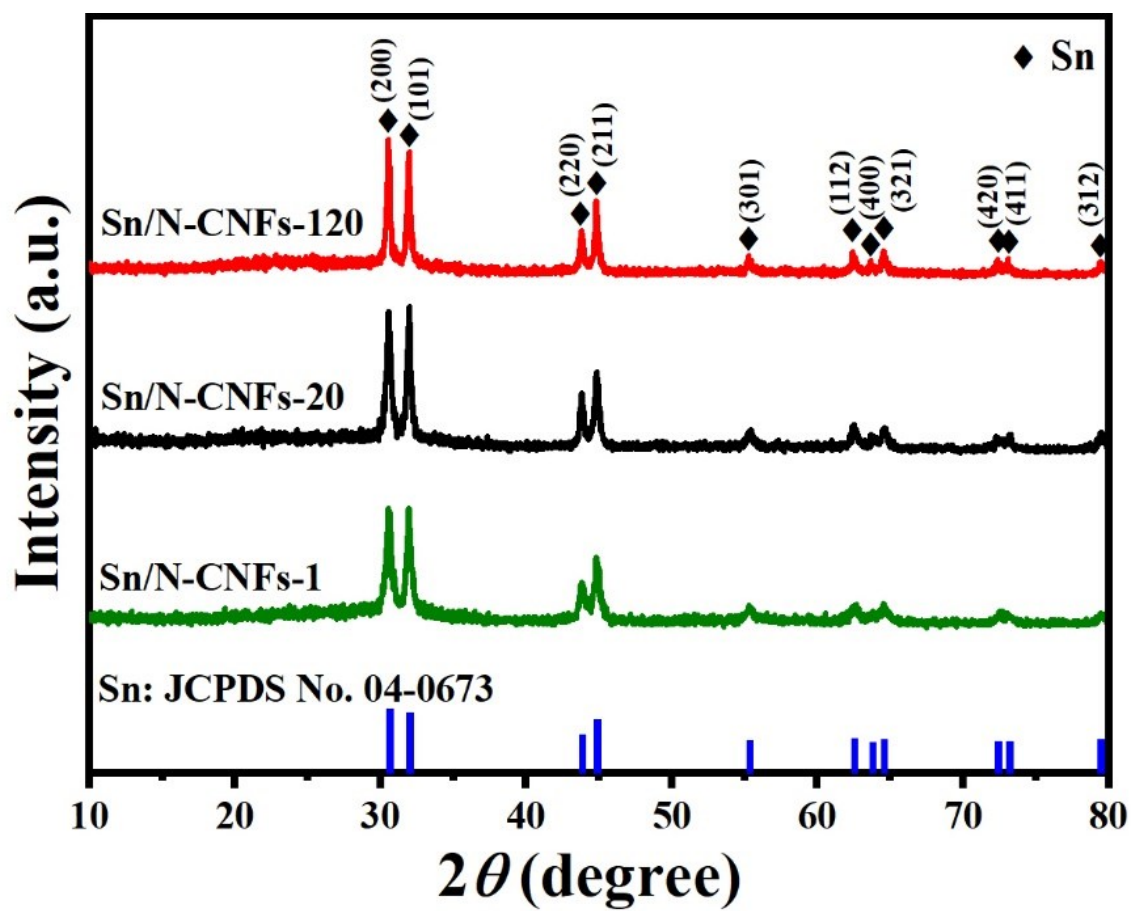


Fig. S2. XRD patterns of Sn/N-CNFs-1, Sn/N-CNFs-20 and Sn/N-CNFs-120.



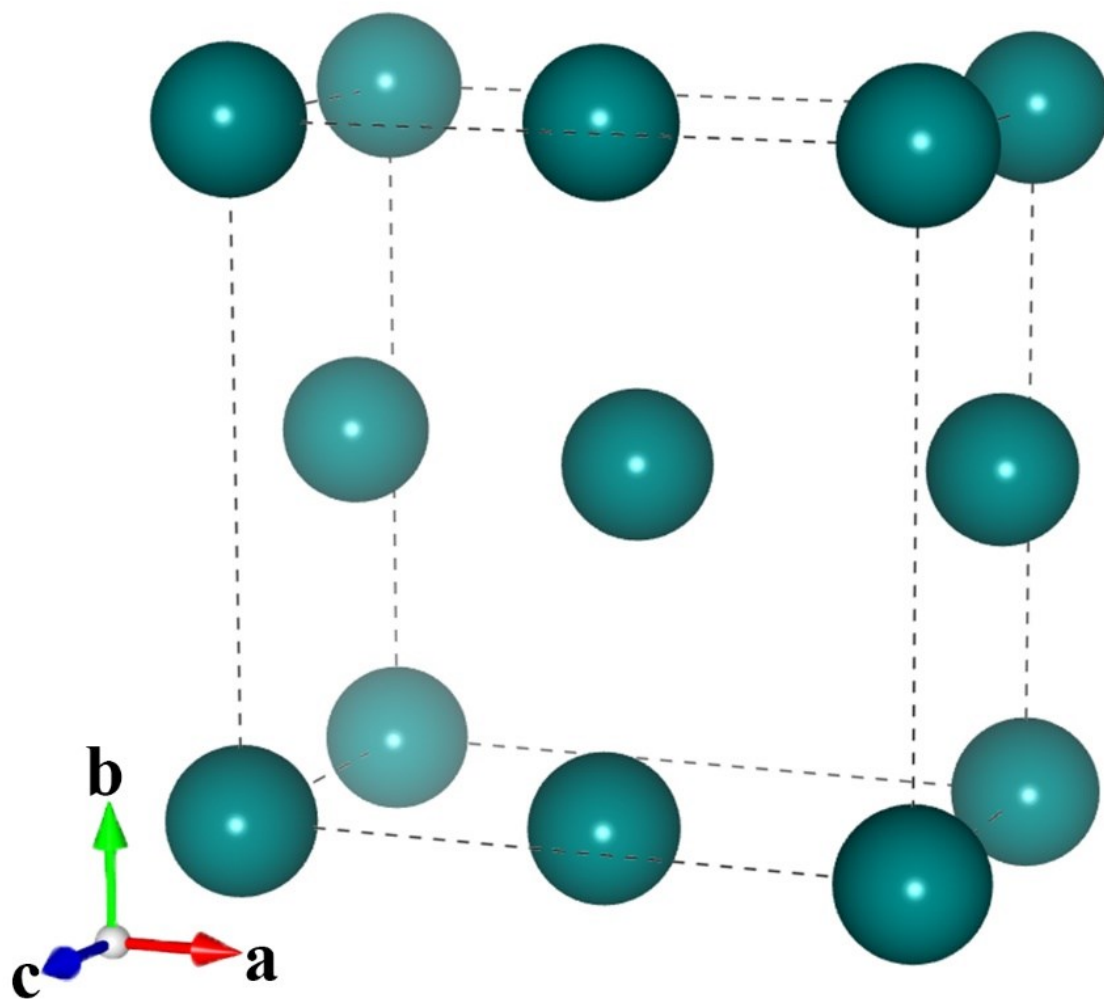


Fig. S3. The crystal structure model of Sn.

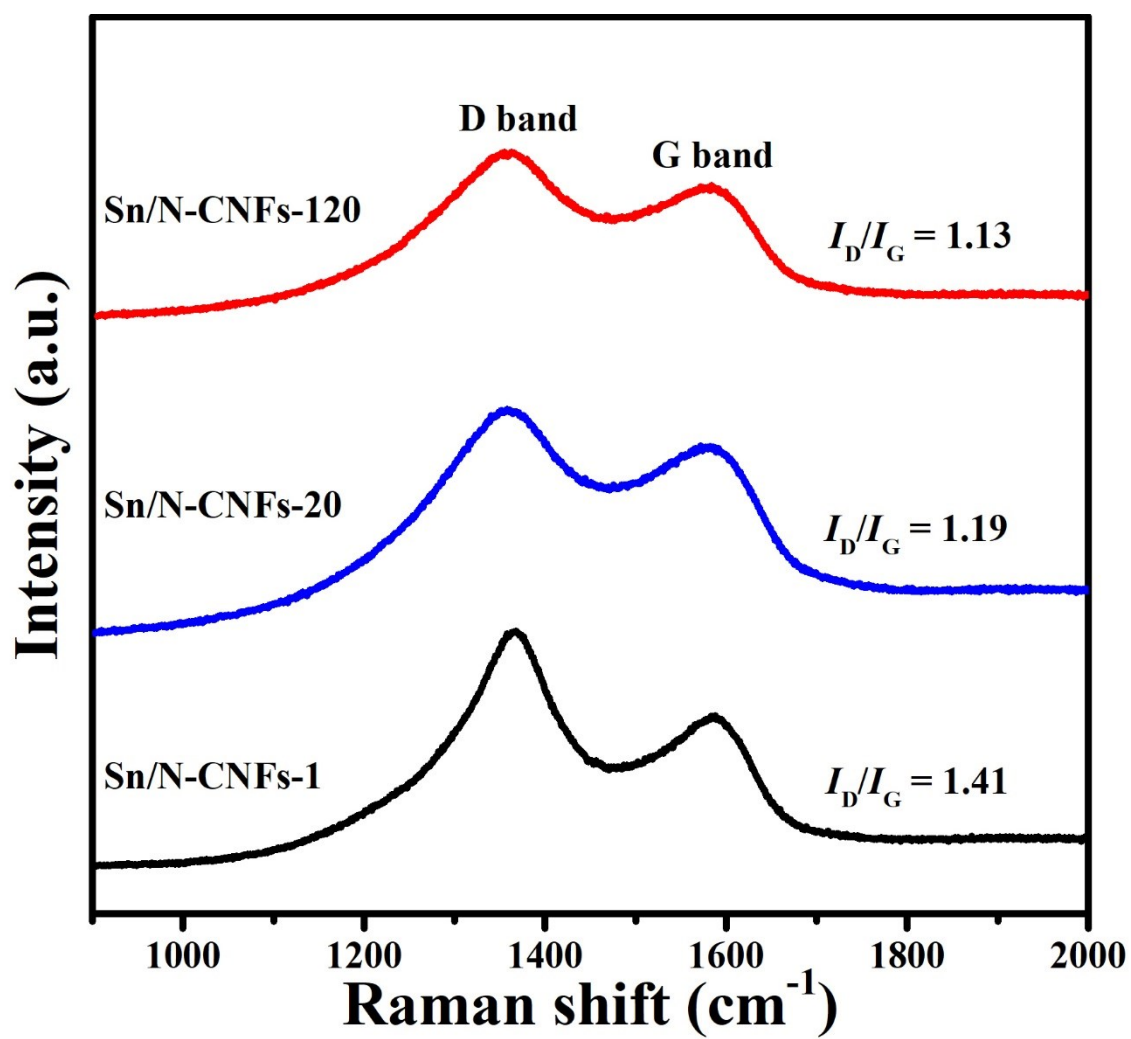


Fig. S4. Raman spectra of Sn/N-CNFs-1, Sn/N-CNFs-20 and Sn/N-CNFs-120.

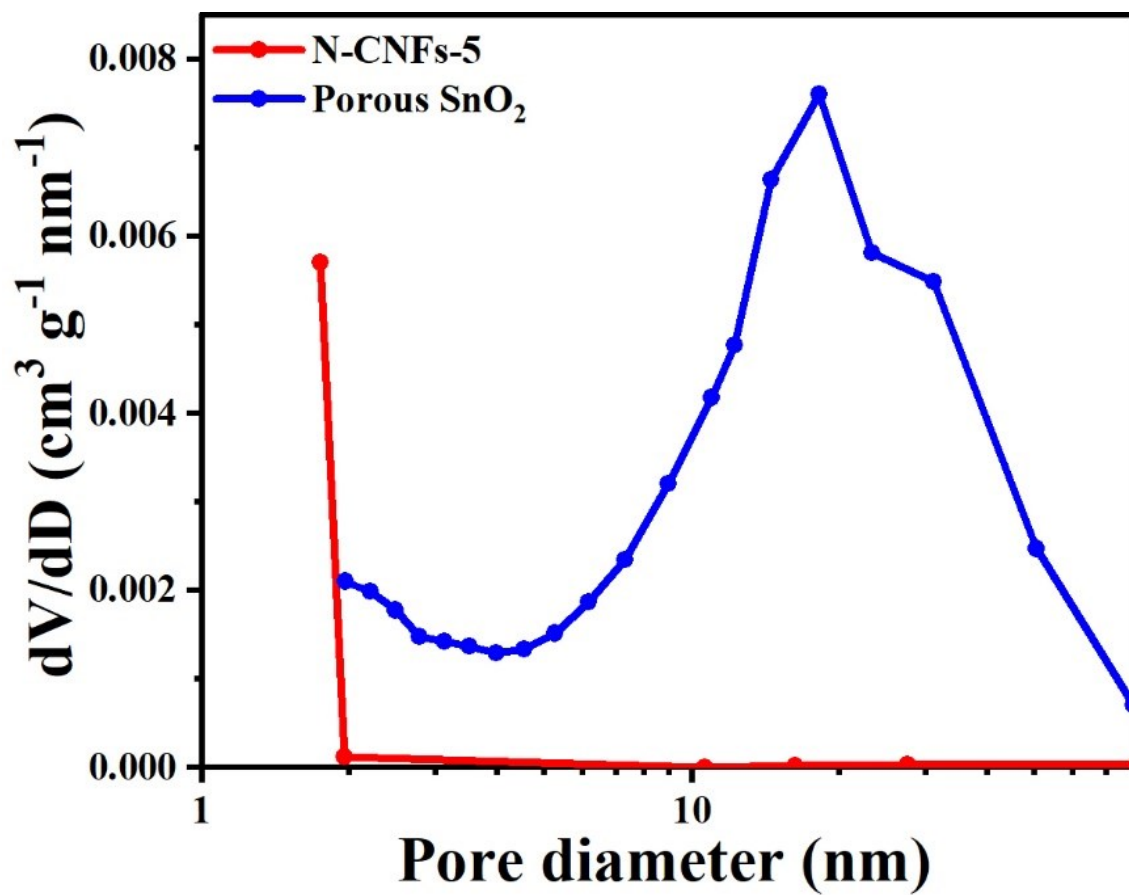
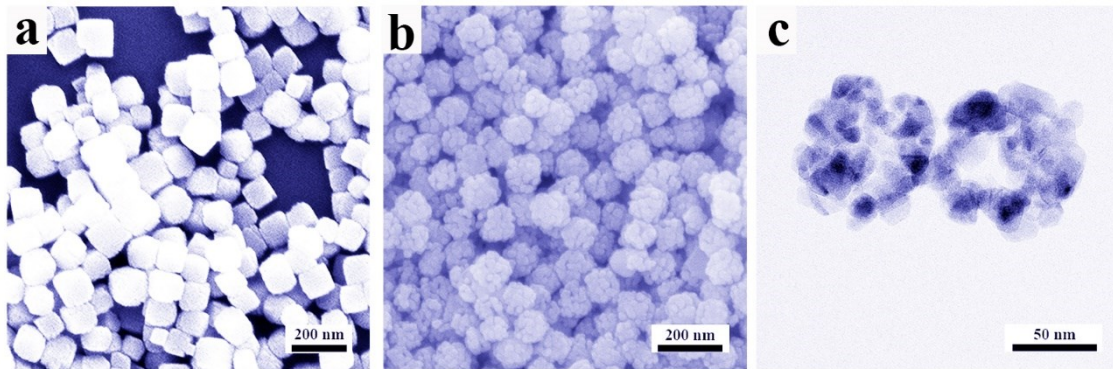
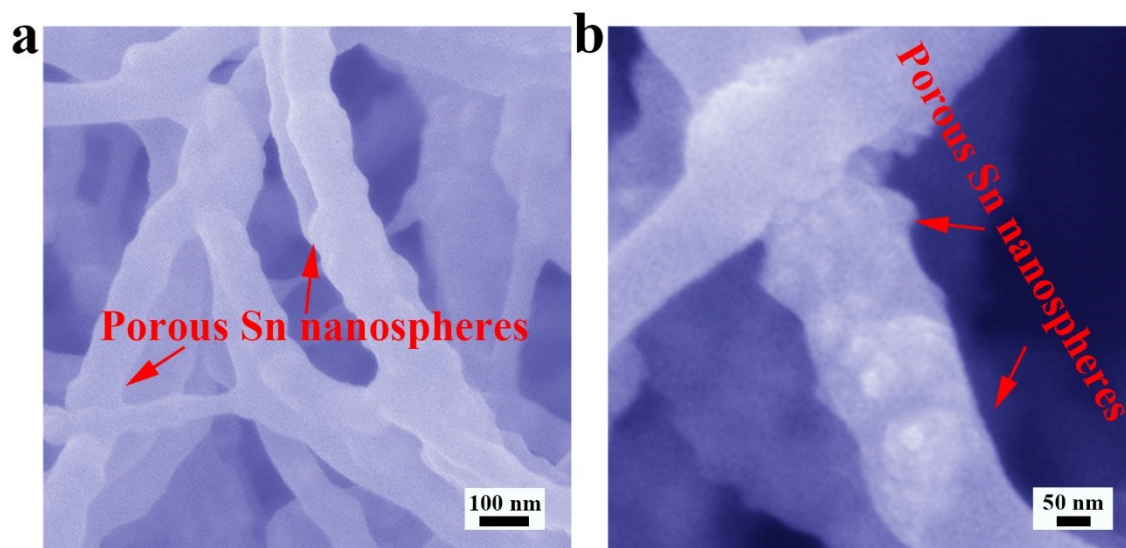


Fig. S5. The pore size distributions of N-CNFs-5 and porous  $\text{SnO}_2$ .



**Fig. S6.** (a) SEM image of  $\text{CoSn(OH)}_6$ , (b) SEM image of  $\text{SnO}_2/\text{Co}_3\text{O}_4$  and (c) TEM image of porous  $\text{SnO}_2$ .



**Fig. S7.** (a) and (b) FESEM images of Sn/N-CNFs-5.

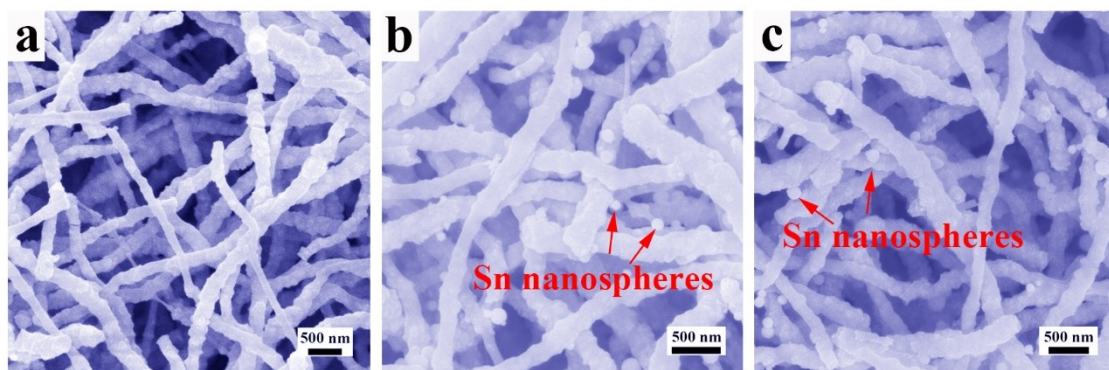


**Fig. S8.** SEM images of (a) Sn/N-CNFs-1, (b) Sn/N-CNFs-20 and (c) Sn/N-CNFs-120.



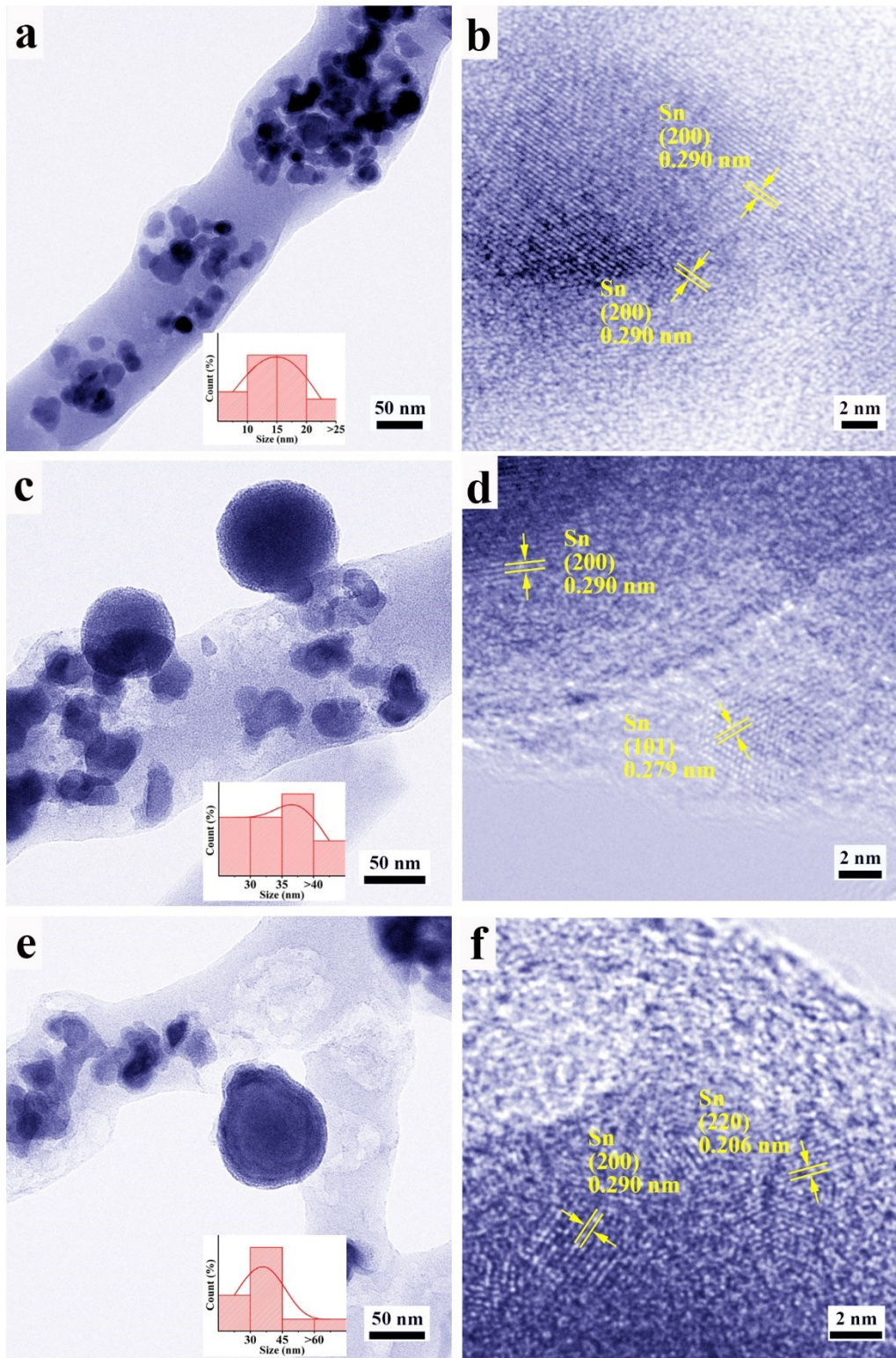


**Fig. S9.** (a) TEM image and particle size distribution (the inset) of Sn/N-CNFs-1. (b) HRTEM image of Sn/N-CNFs-1. (c) TEM image and particle size distribution (the inset) of Sn/N-CNFs-20. (d) HRTEM image of Sn/N-CNFs-20. (e) TEM image and particle size distribution (the inset) of Sn/N-CNFs-120. (f) HRTEM image of Sn/N-CNFs-120.

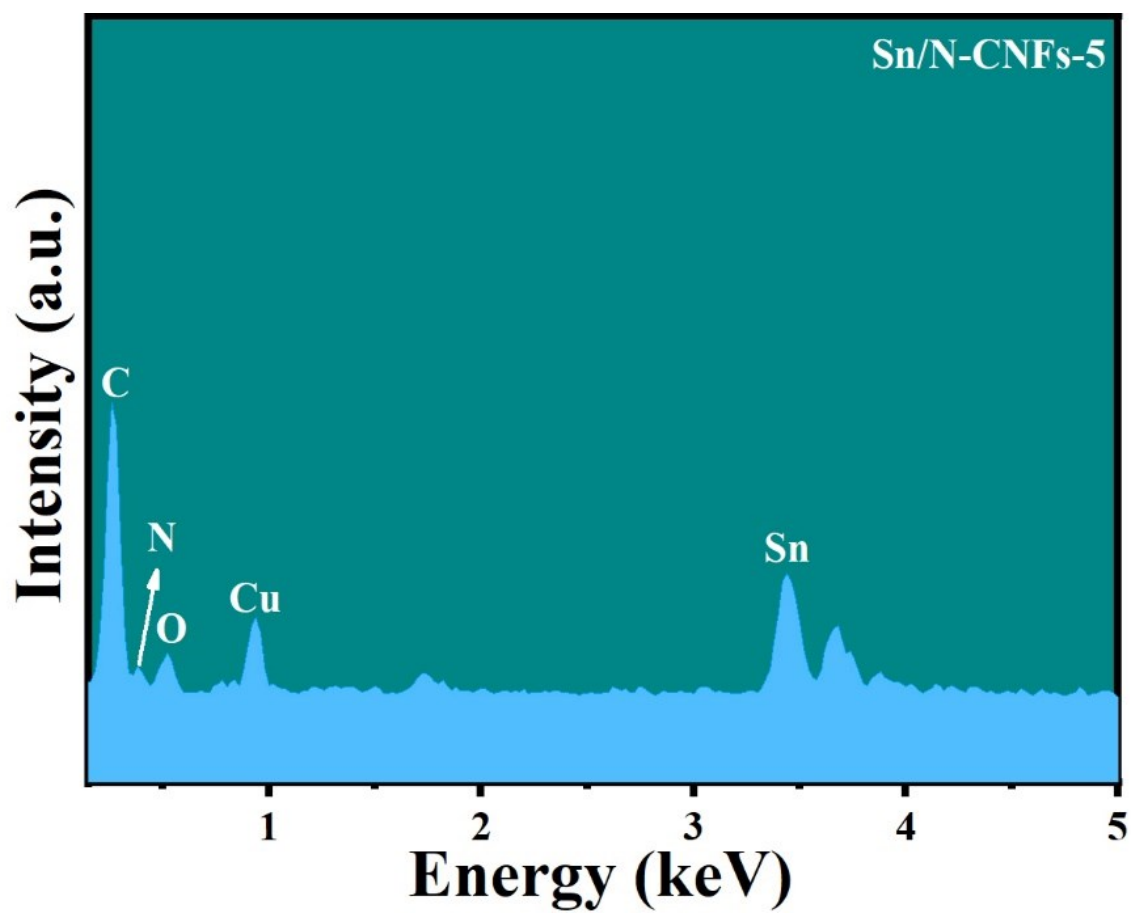
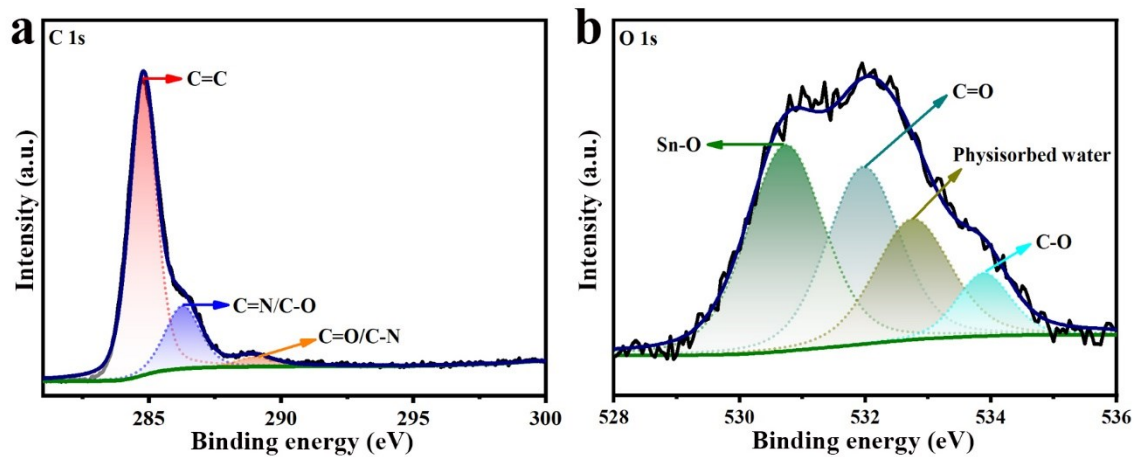
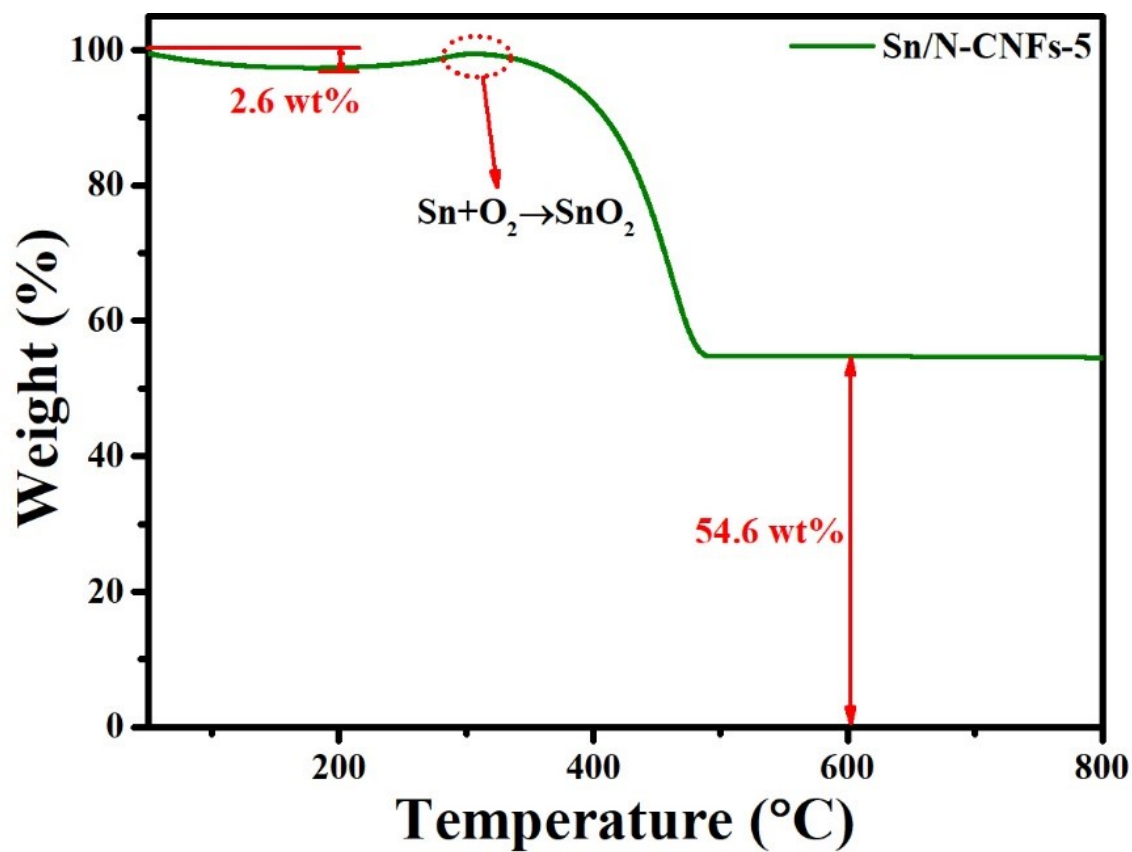


Fig. S10. EDX spectrum of Sn/N-CNFs-5.





**Fig. S11.** High-resolution XPS spectra of (a) C 1s and (b) O 1s of Sn/N-CNFs-5.



**Fig. S12.** TGA curve of Sn/N-CNFs-5. The Sn content in the Sn/N-CNFs-5 hybrid is calculated from:

$$\text{Sn(wt\%)} = \frac{M_{\text{Sn}}}{M_{\text{SnO}_2}} \times \frac{\text{weight of SnO}_2}{\text{weight of Sn/N - CNFs - 5}} \times 100\% = \frac{118.7}{150.7} \times \frac{0.546}{1 - 0.026} \times 100\% = 44.2\%$$

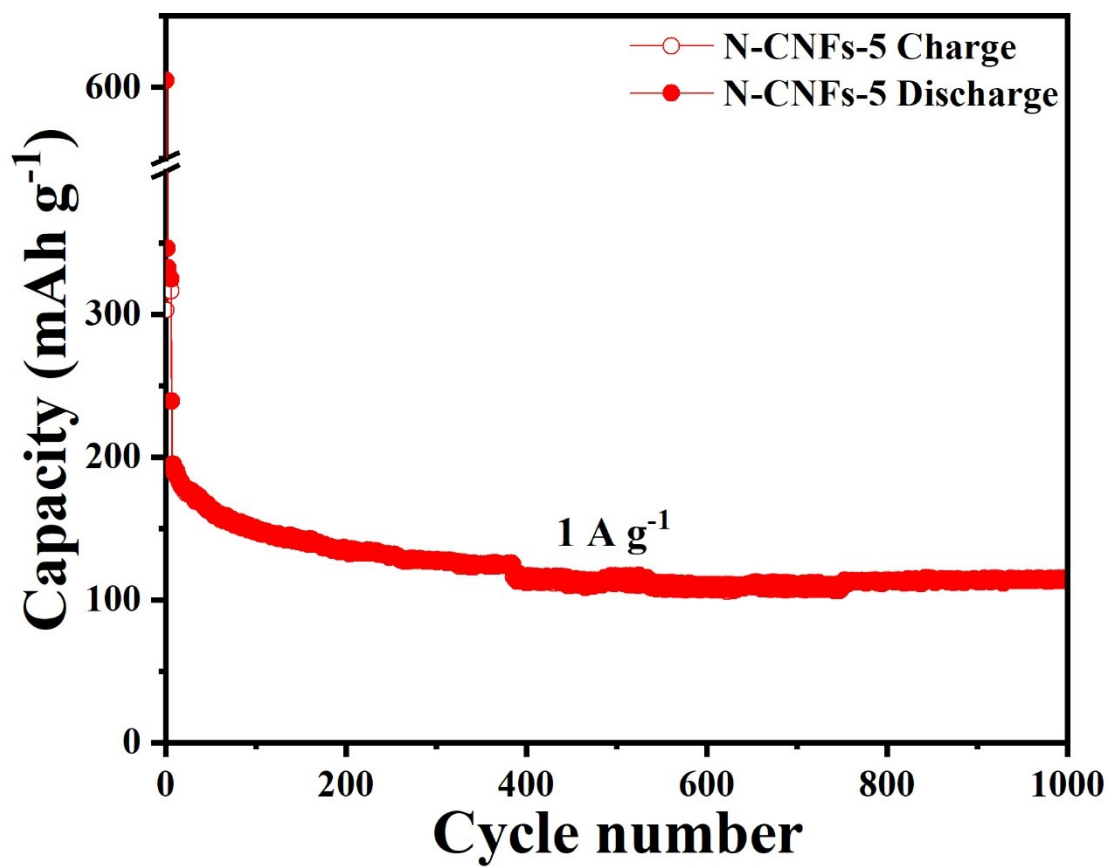
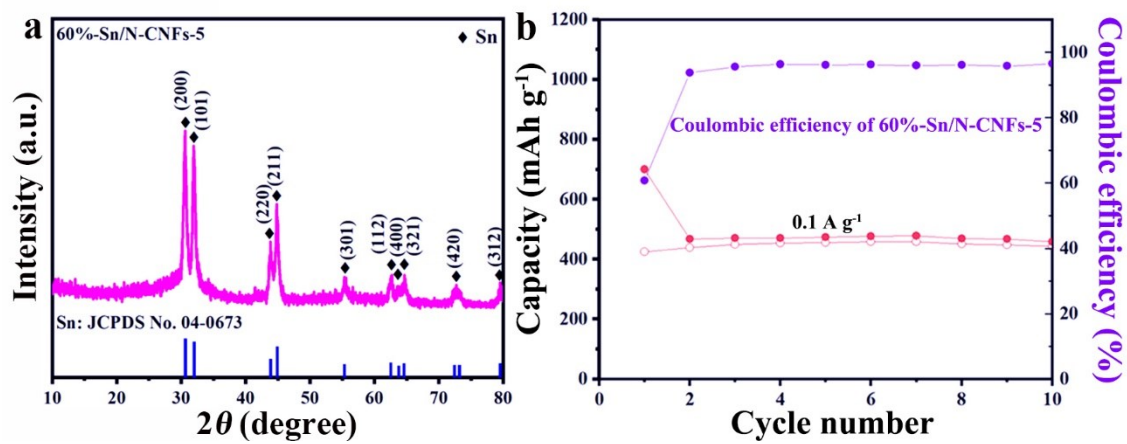
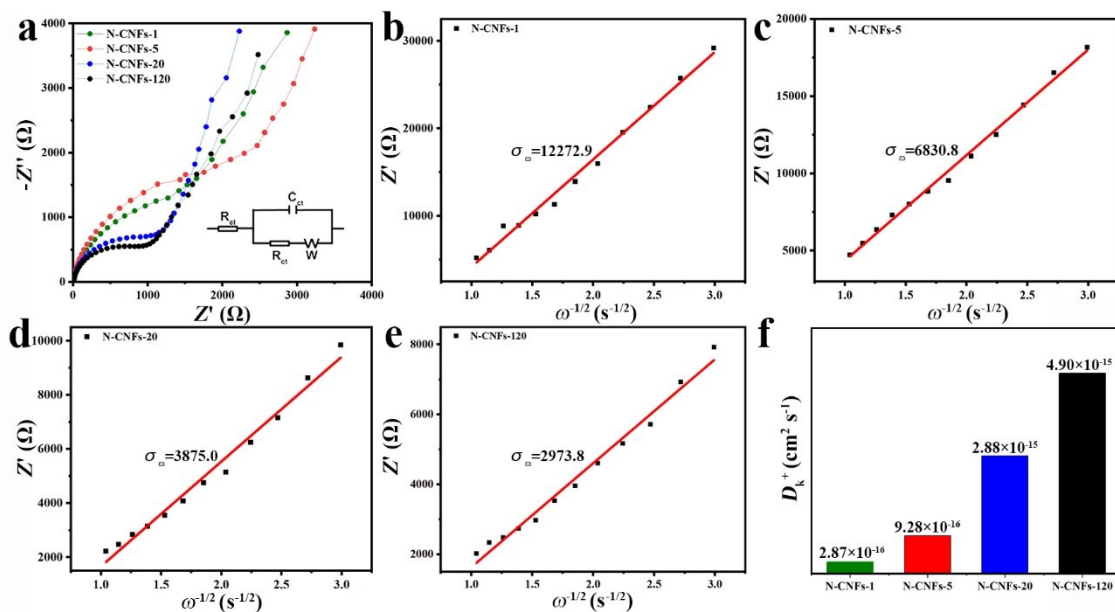


Fig. S13. Cycling performance of the N-CNFs-5 electrode at 1 A g<sup>-1</sup>.



**Fig. S14.** (a) XRD pattern of 60%-Sn/N-CNFs-5. (b) Cycling performance and CE of 60%-Sn/N-CNFs-5 at 0.1 A g<sup>-1</sup>.



**Fig. S15.** (a) EIS plots of the N-CNFs electrodes in fresh PIBs, where the inset shows the equivalent circuit diagram. The linear relationship of  $Z'$  versus  $\omega^{-1/2}$  at low-frequency zone for (b) N-CNFs-1, (c) N-CNFs-5, (d) N-CNFs-20 and (e) N-CNFs-120 electrodes, respectively. (f)  $D_k^+$  values of the N-CNFs electrodes.

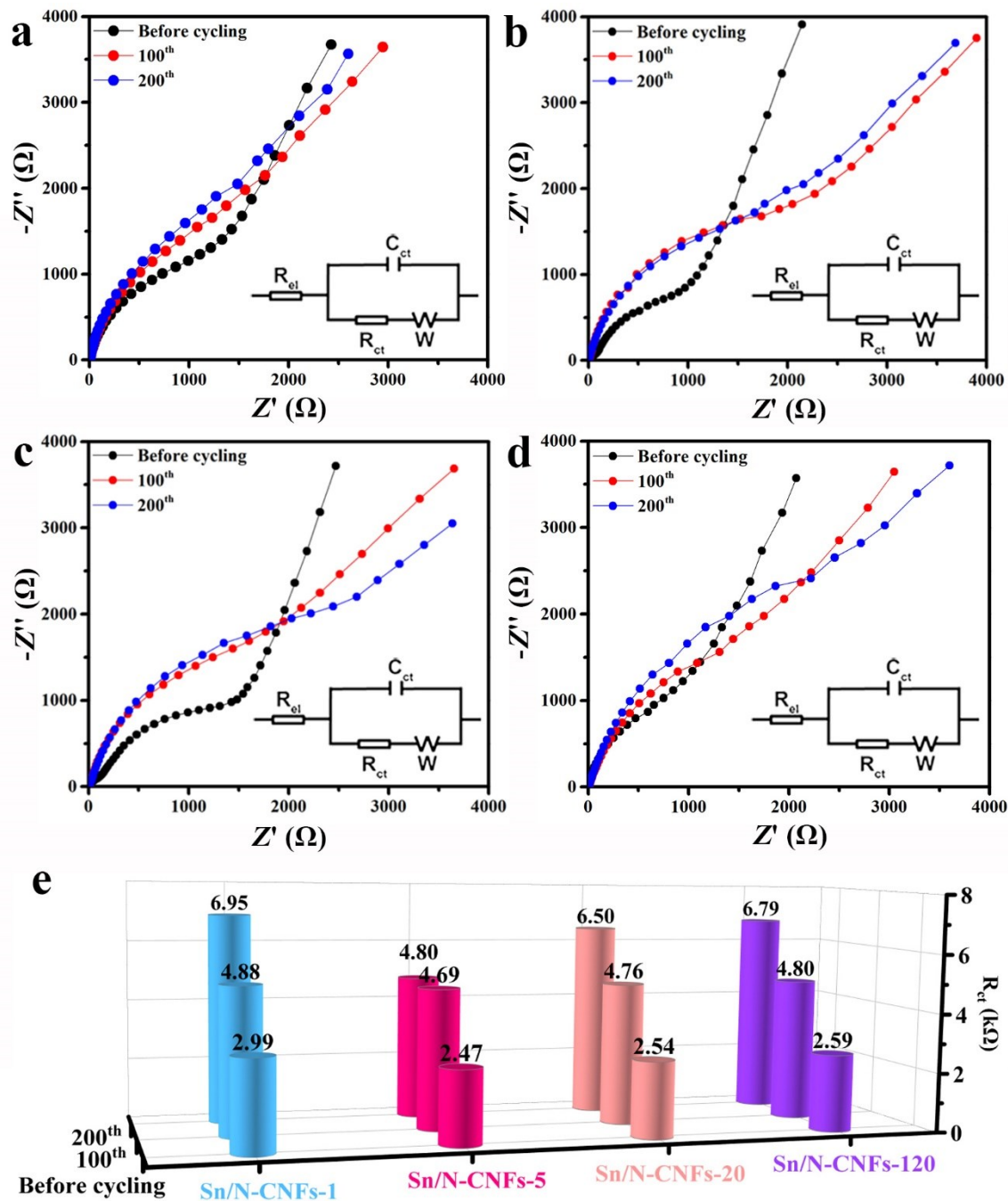


**Fig. S16.** Nyquist plots of (a) Sn/N-CNFs-1, (b) Sn/N-CNFs-5, (c) Sn/N-CNFs-20 and (d) Sn/N-CNFs-120 at different cycles after charging to 3 V at a current density of 0.5 A g<sup>-1</sup>. (e)  $R_{ct}$  values of Sn/N-CNFs-1, Sn/N-CNFs-5, Sn/N-CNFs-20 and Sn/N-CNFs-120 before and after cycling.

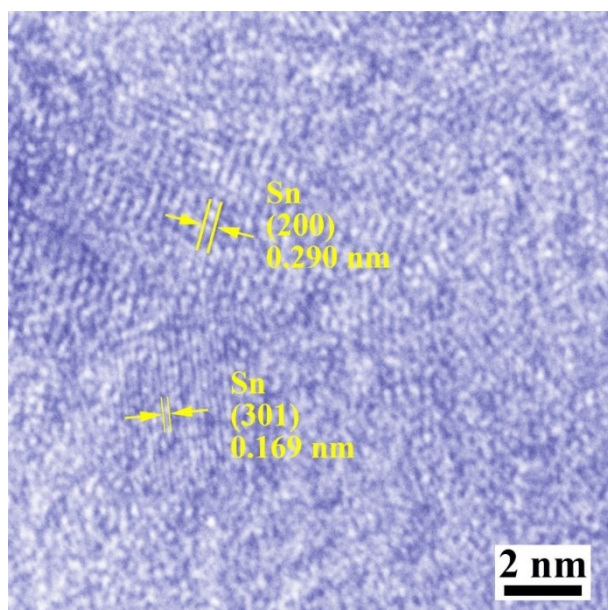


**Fig. S17.** HRTEM image of Sn/N-CNFs-5 after 1000 cycles at 1 A g<sup>-1</sup>.

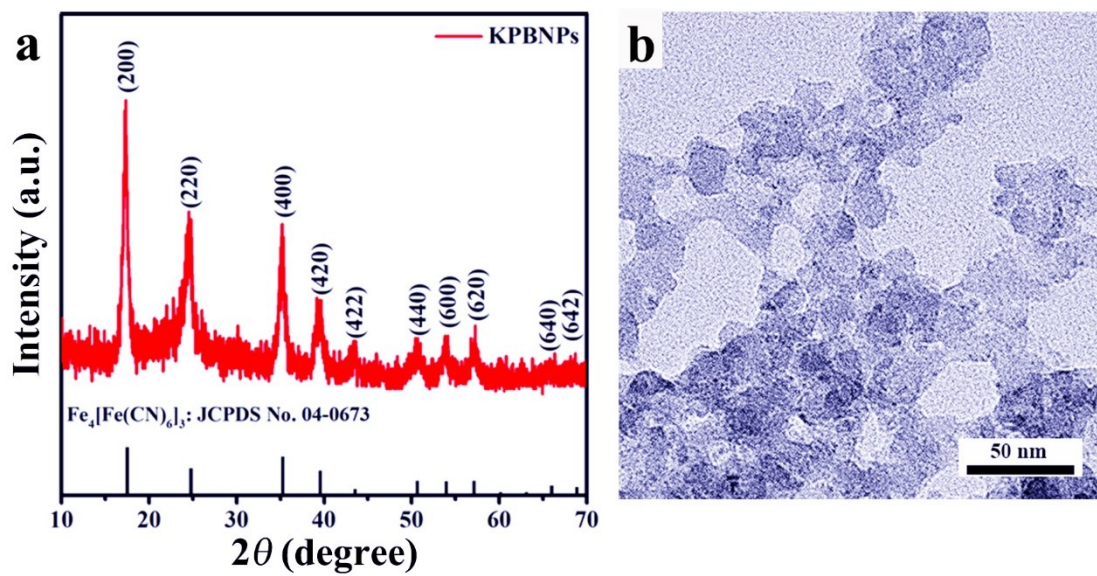


Fig. S18. (a) XRD pattern of KPBNPs. (b) TEM image of KPBNPs.



## Supplementary Tables

**Table S1.** Rate and cycling performances of Sn-based anode materials in PIBs reported in open literatures.

Material	Rate performance	Cycling performance	Ref.
Sn/N-CNFs	168.7 mAh g <sup>-1</sup> (2 A g <sup>-1</sup> )	316.1 mAh g <sup>-1</sup> (100 cycles, 0.1 A g <sup>-1</sup> ) 198.0 mAh g <sup>-1</sup> (3000 cycles, 1 A g <sup>-1</sup> )	This work
Sn/C		≈ 10 mAh g <sup>-1</sup> (50 cycles, 0.05 A g <sup>-1</sup> )	Ref. <sup>[27]</sup> of the txt
Sn-C		110 mAh g <sup>-1</sup> (30 cycles, 0.025 A g <sup>-1</sup> )	Ref. <sup>[25]</sup> of the txt
3D hierarchically porous carbon/Sn	150 mAh g <sup>-1</sup> (0.5 A g <sup>-1</sup> )	276.4 mAh g <sup>-1</sup> (100 cycles, 0.05 A g <sup>-1</sup> )	Ref. <sup>[24]</sup> of the txt
Sn@RGO	67.1 mAh g <sup>-1</sup> (2 A g <sup>-1</sup> )	200 mAh g <sup>-1</sup> (50 cycles, 0.1 A g <sup>-1</sup> ) 123.6 mAh g <sup>-1</sup> (500 cycles, 0.5 A g <sup>-1</sup> )	Ref. <sup>[20]</sup> of the txt
β-Sn		86 mAh g <sup>-1</sup> (50 cycles, 0.023 A g <sup>-1</sup> )	Ref. <sup>[21]</sup> of the txt

## Notes and references

- 1 Z. Liu, R. Guo, J. Meng, X. Liu, X. Wang, Q. Li, L. Mai, *Chem. Commun.*, 2017, **53**, 8284-8287.
- 2 B. Huang, X. Li, Y. Pei, S. Li, X. Cao, R. C. Masse, G. Cao, *Small*, 2016, **12**, 1945-1955.
- 3 C. Zhang, Y. Xu, M. Zhou, L. Liang, H. Dong, M. Wu, Y. Yang, Y. Lei, *Adv. Funct. Mater.*, 2017, **27**, 1604307.